New Method for Introducing Mesopores into Carbon Microhoneycombs Using Dextran

Shinichiroh Iwamura*, Kohei Kitano, Isao Ogino, Shin R. Mukai

Graduate School of Engineering, Hokkaido University

N13W8, Kita-ku, Sapporo 060-6828, Japan

*Corresponding author. N13W8, Kita-ku, Sapporo 060-6828, Japan

E-mail address: iwamura@eng.hokudai.ac.jp (S. Iwamura)

Fax: +81-11-706-6593 (S. Iwamura)

ABSTRACT

Carbon microhoneycombs (CMHs), which can be prepared from a resorcinol–formaldehyde (RF) hydrogel using ice crystals as a template, are attractive materials for industrial applications such as solid catalysts and adsorbents in flow system reactors. For such applications, pores in a material are important for mass transfer, but the mesopore volumes of CMHs are smaller than that of typical RF-derived carbons because ice crystals compress RF gels during freezing, and mesopores partly collapse. The introduction of mesopores into CMHs requires an additional step such as HCl treatment in the preparation process, and this increases the preparation time. In this work, we developed a convenient method for introducing mesopores into CMHs, in which dextran was added to the initial RF solution. This simple step increased the mesopore volume from 0.015 to 0.191 cm^3/g. We investigated the porous structure of the sample at each step in the preparation, and found that dextran protected the porous structure of the RF hydrogel from growth of ice crystals, enabling mesopore introduction. A combination of dextran addition and HCl treatment further increased the mesopore volume to 0.753 cm^3/g; this cannot be achieved using HCl treatment alone. This may be because the HCl solution can diffuse through the mesopores introduced by dextran addition, and this promotes pore formation.

Keywords: Mesoporous material; Ice-templating method; Porous carbon; Adsorbent; Catalyst support

1. Introduction

Porous carbons are useful functional materials for various applications such as adsorbents [1-4], electrode materials [5-9], and catalyst supports [10-14]. Carbon gels have attracted interest because they can be prepared as monoliths, and their pore sizes can be tuned in the micro- to meso-pore range. Carbon gels are prepared by carbonization of resorcinol–formaldehyde (RF) gels, which have porous structures and shapes that can be easily controlled by adjusting the preparation conditions [15-18]. Carbon gels inherit their porous structures and shapes from the parent RF gel; therefore, carbon gels with various shapes and porous structures can be prepared [6, 7, 16, 17, 19, 20]. For some applications, micropores can be introduced into carbon gels by physical [6, 7, 20-22] or chemical [23, 24] activation after carbonization.

The morphology (macrostructure) of a carbon gel can be controlled by molding the parent RF hydrosol. One of many molding methods is the ice-templating method, in which an RF hydrosol is frozen to separate ice crystals and solid components, and is then dried to remove the ice crystals. This method is environmentally friendly and requires only simple apparatus. Various structures such as sponges, fibers, lamellae, and honeycombs can be formed, depending on the preparation conditions [25, 26]. The honeycomb structure has potential industrial applications, e.g., in flow-type reactors,

because the macrochannels cause minimal pressure drops and the thin honeycomb walls shorten mass transfer distances. Such micro-ordered straight channels are smaller than those obtained using other methods such as extrusion molding. Our group has used carbon materials with honeycomb structures as absorbents [27] and solid catalysts [14].

In these applications, the mesopores in the walls of carbon microhoneycombs (CMHs) improve mass transfer of adsorbates or reactants, respectively. Mesopores need to be introduced into CMHs to improve their efficiency in such applications. In the ice-templating method, growth of ice rods compresses the RF gels containing mesopores, and some mesopores collapse. Due to this, the mesopore volumes in the resulting CMHs tend to be smaller than that of typical carbon gels. This tendency is particularly evident in the RF hydrogels with small mesopores, prepared at a higher concentration of a polymerization catalyst.

In previous studies, mesopores were introduced into carbon gels using HCl treatment, in which an RF hydrogel is aged in HCl solution. This method can be used to introduce mesopores into RF hydrogels whose mesopores have partly collapsed because of ice-rod growth [14, 27]. HCl treatment is a useful technique but aging is a time-consuming process. Our group reported an increase in the mesopore volume of a

CMH from 0.07 to 0.61 cm^3/g, for an aging time of 14 d [27]. In addition, there is a limit to the increase in the mesopore volume that can be achieved using HCl treatment alone. For some applications, a new method is needed for increasing the mesopore volumes in porous monoliths prepared using the ice templating method, even at conditions in which mesopores easily collapse.

In this work, we developed a new method for introducing mesopores into CMHs using an additive. For an additive into the initial solution, polymers and saccharides are candidate because they wouldn't undesirably affect growth of ice-crystal and sol-gel reaction. And low-cost and environmental-friendly materials such as saccharides are preferable. We found that dextran shows the effect among some saccharides. Dextran molecules can disperse in an RF hydrogel and protect its porous framework from growth of ice rods. This method simply involves mixing dextran with a precursor RF sol. We clarified the effects of dextran addition by comparing CMHs prepared using different amounts of dextran and samples prepared with the other saccharide additions. We also showed that this method can be used along with the conventional HCl treatment to further increase the mesopore volume.

2. Experimental

2.1. Sample preparation

Resorcinol (99%), formaldehyde (36 wt% aqueous solution with 7% methanol as stabilizer), dextran (M_w = 40 000), glucose (98%, D-glucose), dextrin (dextrin hydrate), sodium carbonate (99.5%), *tert*-butyl alcohol (TBA, 99%), and 1 N HCl were purchased from Wako Pure Chemical Industries Ltd in Japan.

CMHs were prepared using the method reported in the literature [14, 27], but with dextran addition. An initial solution was prepared by mixing resorcinol (R), formaldehyde (F), dextran (D), sodium carbonate (C), and water (W), in the following ratios: R/C = 50 (mol/mol), R/F = 0.5 (mol/mol), R/W = 0.1 (mol/mL), and D/R = 0–0.5 (g/g). The solution was placed in a tubular glass mold [50 mm × 8 mm (i.d.)] and kept at 30 °C for 10 h to obtain an RF hydrogel through gelation and aging. The hydrogel was washed with excess water to remove unreacted formaldehyde. It was confirmed that dextran in the hydrogel is hardly dissolved by this washing. The RF hydrogel was loaded into a propylene test tube [125 mm × 13 mm (i.d.)] and unidirectionally dipped in a liquid-nitrogen bath at a rate of 60 mm/h to obtain an RF microhoneycomb (RFMH). The frozen RFMH was thawed, removed from the test tube and immersed in excess TBA for 1 d to exchange water in the sample with TBA. The resulting sample was freeze-dried at −10 °C for 3 d. The dried RFMH was carbonized at 500 °C for 4 h in a N_2 flow of 100 mL/min, using a tubular reactor [21 mm (i.d.)], to obtain a CMH. In some

experiments, a sample was thawed after unidirectional freezing and aged in excess 1 N HCl solution for a fixed time (4–14 d). Samples are denoted by CMH-(D/R ratio)-(aging time in days in HCl solution); for example, CMH-0.5-4 denotes the CMH prepared at a D/R ratio of 0.5 with HCl treatment for 4 d. In addition, samples were also prepared with glucose and dextrin addition. Their preparation condition was almost the same as CMH-0.5-0 with only modifying the additive from dextran to glucose or dextrin.

2.2. Characterization

The sample morphologies were examined using scanning electron microscopy (SEM; JEOL JSM-5410). The nanostructures of the CMHs were examined at high magnification using field-emission SEM (FE-SEM; JEOL JSM-6500F). The sample porous structures were investigated using N_2 adsorption/desorption (BELSORP-mini II, Microtrac BEL Corp.) at −197 °C, after drying at 250 °C for 4 h under a N_2 flow. When the porous structures of non-carbonized samples (RF and RFMH) were examined, drying was performed at a lower temperature, i.e., 150 °C, for 12 h to avoid sample decomposition. In these cases, the sample weight was determined from the estimated weight after carbonization, using the carbon yield (ca. 55%), for comparison with the carbonized sample. The relative surface areas and mesopore size distributions were calculated using the Brunauer–Emmett–Teller (BET) method and the Dollimore–Heal

(DH) method, respectively. The micropore volumes (V_{micro}) and total pore volumes (V_{total}) were calculated using the Dubinin–Radushkevich (DR) method and determined from the N_2 uptakes at $P/P_0 = 0.96$, respectively. The mesopore volumes (V_{meso}) were estimated by subtracting V_{micro} from V_{total}.

3. Results and discussion

3.1. CMH morphologies

CMHs were prepared using a low carbonization temperature toward applications using surface functional groups on the CMH surface. In spite of the low carbonization temperature, the obtained CMHs are black and weight loss during carbonization is almost the same with that of a high carbonization temperature. Figure 1 shows SEM images of CMHs prepared using various amounts of dextran (various D/R values). The images show that each sample has a honeycomb structure, indicating that straight ice rods grow even if dextran is added. The channel sizes of CMH-0.25-0 and CMH-0.5-0 are slightly smaller than that of CMH-0-0. These decreases in the channel sizes are in agreement with the results of our previous study, in which dextran addition decreased the ice-rod size at unidirectional freezing [28].

3.2. CMH porous structures

Figure 2 shows the N_2 adsorption isotherms and the pore size distributions of CMHs prepared using various amounts of dextran. Their pore size distributions were calculated using the DH method. Fig. 2a shows that the N_2 uptakes of all the samples at a low relative pressure, i.e., less than 0.1, are almost the same. The data in Table 1 show that the BET surface areas (S_{BET}) and micropore volumes (V_{micro}) of all the sample are almost the same, regardless of dextran addition. These results indicate that dextran addition hardly affects the CMH microporous structure. In contrast, the N_2 uptakes at relative pressures from 0.4 to 0.9 for CMHs prepared with dextran addition are larger than that of CMH-0-0. In this preparation condition, mesopores easily collapse, but this result clearly shows that simply adding dextran introduces mesopores. Table 1 also shows that the mesopore volume (V_{meso}) increases with increasing amount of added dextran. The pore size distributions in Fig. 2b show that the CMHs prepared with dextran addition have many pores of size 5–20 nm, but the mesopore volume of the CMH prepared without dextran addition largely decreases. The peaks in the CMH-0.25-0 and CMH-0.5-0 pore size distributions are almost the same (5.3 and 6.1 nm, respectively). It can therefore be concluded that the amount of dextran added slightly affects the mesopore size in the resulting CMHs, and greatly affects the mesopore volume.

3.3. Effect of added saccharides

To investigate effect of added saccharides, samples were prepared with glucose and dextrin addition. Their SEM images and N_2 adsorption isotherms are shown in Fig. 3 and Fig. 4, respectively. The sample prepared with glucose addition is honeycomb structure and its porous structure is almost the same as CMH-0-0, indicating glucose doesn't affect the porous structure. The sample prepared with dextrin addition is a lamella structure and the N_2 uptake largely decreases. Dextrin molecule contains branched-chain consisting of α-1,4 and 1,6 glycosidic linkages more than dextran molecule, which is mainly constructed from straight chain consisting of α-1,6 glycosidic linkages. Such dextrin molecule would affect sol-gel reaction of RF hydrogel and ice growth. These results indicate that dextran is a certain molecular size and structure to introduce mesopores into CMHs.

3.4. Mechanism of mesopore introduction

Next, we discuss the mechanism of mesopore introduction by dextran addition. Generally, the mesopores in carbon gels exist as voids between carbon nanoparticles; the carbon nanoparticles aggregate to form a carbon gel powder or monolith [15, 17, 18]. High-resolution FE-SEM was used to investigate the effect of dextran addition on the CMH particle size. Figure 5 shows FE-SEM images of CMH-0-0, CMH-0.25-0, and

CMH-0.5-0. The images are not very clear because of the high magnification, but they show that the particles from which all the CMHs are constructed are of similar sizes, i.e., around 9 nm. This shows that dextran addition did not affect the nanoparticle preparation step during the sol–gel reaction of the RF hydrosols. After carbonization, the diameters of the carbon nanoparticles forming each CMH are the same. The inter-particle spaces of such small particles are smaller than mesopores, therefore the initial sol–gel reaction for nanoparticle construction is not involved in the introduction of mesopores by dextran addition. The introduced mesopores therefore come from a secondary structure of the carbon nanoparticles. Mesopore construction involves one of the following processes: 1. a sol–gel process, 2. unidirectional freezing, 3. drying, and 4. carbonization. We investigated mesopore construction by examining the porous structures of the samples at each preparation step, with and without dextran addition.

N_2 adsorption experiments were performed using samples obtained before unidirectional freezing (RF-0-0 and RF-0.5-0) and before carbonization (RFMH-0-0 and RFMH-0.5-0) during the preparations of CMH-0-0 and CMH-0.5-0. The samples obtained before unidirectional freezing were freeze-dried after exchanging water with TBA. During carbonization, the sample structures slightly change but the sample weights largely decrease. When isotherms based on the sample weight are compared,

the N_2 uptake of the carbonized samples looks large (see Supplementary information). To compare the pore volumes of the structures, the amounts of adsorbed N_2 were calculated based on the weight estimated from their carbon yields. The isotherms based on the calculated sample weight are shown in Fig. 6 together with those for CMH-0-0 and CMH-0.5-0. In the cases of the samples prepared without dextran addition (Fig. 6a), RF-0-0 adsorbs large amounts of N_2 across a wide relative pressure region, which indicates the presence of many mesopores. After unidirectional freezing, little N_2 is adsorbed by RFMH-0-0 at all relative pressures, meaning that many pores in the sample have collapsed. Figure 7a shows the structural changes that occur during unidirectional freezing of a typical hydrogel. Ice rods grow from the bottom to the top and solid components are concentrated between the ice rods to form honeycomb walls. Pores in the RF hydrogel are then compressed and partly collapse. This mechanism probably results in the decrease in the sample mesopore volume. After carbonization, the sample mesopore volume is small, because the nanostructure of the RF resin is maintained, although micropores are introduced. For the samples prepared with dextran addition, the mesopore volume of RF-0.5-0 is smaller than that of RF-0-0, indicating that dextran molecules disperse in the RF gel and close the pores. After unidirectional freezing, the mesopore volume is mostly maintained, although the shape

of the isotherm changes slightly. These results suggest that dextran addition protects the porous structure from growth of ice rods. After carbonization, the mesopores are mostly retained, together with an increase in the micropore volume. Based on these results, the mechanism of mesopore introduction by dextran addition can be summarized as shown in Fig. 7b. When the hydrogel is prepared, dextran molecules are dispersed in the RF network and support the porous structure using their straight chain. These supports protect the porous structure from pressure caused by growth of ice rods; therefore, many mesopores are retained after unidirectional freezing and carbonization. On the other hand, small molecules like glucose couldn't protect the porous structure and the mesopore volume largely decreased from the pressure caused by ice-growth.

3.5. Combination of dextran addition and HCl treatment

The mechanism discussed in the last section shows that mesopores are introduced by dextran addition through a different process from that in conventional HCl treatment. This suggests that combining dextran addition with HCl treatment would further increase the CMH mesopore volume. We prepared CMHs using dextran addition along with HCl treatment for 4 d to obtain CMHs with larger mesopore volumes. The N_2 adsorption isotherms and pore size distributions of the CMHs are

shown in Fig. 8. HCl treatment clearly increases the amount of N_2 adsorbed by each CMH at low relative pressures, i.e., below 0.2. Regardless of the amount of dextran added, their S_{BET} and V_{micro} values are twice those of the CMHs prepared without HCl treatment (Table 1). This means that HCl treatment affects the microporous structures of the RF hydrogels even in the presence of dextran. The isotherm for CMH-0-4 shows N_2 uptake at relative pressures between 0 and 0.8, and its mesopore volume increases (to 0.28 cm^3/g) compared with that of CMH-0-0 (0.02 cm^3/g). For the samples prepared with dextran addition, the N_2 uptakes at relative pressures between 0 and 0.8 are further increased by HCl treatment. Their mesopore volumes increase from 0.14 to 0.48 (CMH-0.25-4) and from 0.20 to 0.79 (CMH-0.5-4). The mesopore volumes of CMH-0-4, CMH-0.25-4, and CMH-0.5-4 increase by 0.26, 0.34, and 0.59 cm^3/g, respectively, showing that the efficiency of the HCl treatment increases with increasing dextran addition. The pore size distributions in Fig. 8b show that the CMH-0-4 pores are smaller than those of CMH-0.25-4 and CMH-0.5-4, although that of CMH-0-4 is greater than that of CMH-0-0. The effect of dextran addition suggests that mesopores had already been introduced into the sample by dextran addition when HCl treatment of the sample started. The HCl solution can homogeneously diffuse through the sample via the mesopores formed by dextran addition. The diffused HCl solution can effectively

promote formation of additional mesopores by Ostwald ripening. Different volumes of mesopores can therefore be introduced into CMHs for the same treatment time, depending on the amount of dextran added (i.e., the mesopore volume already introduced). In the case of the CMH prepared without dextran addition, the HCl solution hardly diffuses through the sample because of the small pore size and volume. The mesopore volume of CMH-0-4 is therefore smaller than those of CMH-0.25-4 and CMH-0.5-4.

HCl treatment introduce mesopores, and the volume increases with increasing treatment time [27, 29]. The isotherm and pore size distribution of a CMH prepared using lengthy HCl treatment (CMH-0-14) is shown in Fig. 8. The figure confirms that the mesopore volume and pore size of CMH-0-14 are much higher than those of CMH-0-4. However, the mesopore volume of CMH-0-14 is smaller than that of CMH-0.5-4. These results suggest that a combination of dextran addition and HCl treatment effectively introduces mesopores, but there is a limit to the amount of mesopores introduced by HCl treatment alone. These results show that the combination method not only shortens the preparation time, but also introduce larger amounts of mesopores.

4. Conclusions

In this work, we developed a new technique for introducing mesopores into monolithic porous carbon with a honeycomb structure (CMH). The CMH was prepared from an RF hydrogel using the ice-templating method. CMHs have potential applications as catalyst supports and adsorbents in flow systems, in which mesopores are important for effective mass transfer. This technique simply involves mixing a typical saccharide, i.e., dextran, into the initial solution. It is more effective for introducing mesopores into CMHs than the previous technique, HCl treatment. Dextran addition can be combined with HCl treatment to introduce additional mesopores. Our investigation suggests that the mechanism of mesopore introduction is that dextran protects the porous structure of the RF gel from pressure caused by ice-rod growth during unidirectional freezing. This technique could be used to prepare porous materials by the ice-templating method not only from RF hydrogels, but also from various other starting materials.

References

[1] R.V. Siriwardane, M.S. Shen, E.P. Fisher, J.A. Poston, Energy & Fuels, 15 (2001) 279-284.
[2] A. Dabrowski, P. Podkoscielny, Z. Hubicki, M. Barczak, Chemosphere, 58 (2005) 1049-1070.
[3] P.K. Malik, Dyes and Pigments, 56 (2003) 239-249.
[4] C. Namasivayam, D. Kavitha, Dyes and Pigments, 54 (2002) 47-58.
[5] A.G. Pandolfo, A.F. Hollenkamp, J. Power Sources, 157 (2006) 11-27.
[6] H. Probstle, M. Wiener, J. Fricke, J. Porous Mater., 10 (2003) 213-222.

[7] R.W. Pekala, J.C. Farmer, C.T. Alviso, T.D. Tran, S.T. Mayer, J.M. Miller, B. Dunn, J. Non-Cryst. Solids, 225 (1998) 74-80.
[8] H. Nishihara, T. Kyotani, Adv. Mater., 24 (2012) 4473-4498.
[9] J. Li, X. Wang, Q. Huang, S. Gamboa, P.J. Sebastian, J. Power Sources, 158 (2006) 784-788.
[10] J.S. Yu, S. Kang, S.B. Yoon, G. Chai, J. Am. Chem. Soc., 124 (2002) 9382-9383.
[11] G.S. Chai, S.B. Yoon, J.S. Yu, J.H. Choi, Y.E. Sung, J. Phys. Chem. B, 108 (2004) 7074-7079.
[12] S. Zhang, L. Chen, S. Zhou, D. Zhao, L. Wu, Chem. Mater., 22 (2010) 3433-3440.
[13] N. Narischat, T. Takeguchi, T. Tsuchiya, T. Mori, I. Ogino, S.R. Mukai, W. Ueda, Journal of Physical Chemistry C, 118 (2014) 23003-23010.
[14] K. Murakami, Y. Satoh, I. Ogino, S.R. Mukai, Industrial & Engineering Chemistry Research, 52 (2013) 15372-15376.
[15] R.W. Pekala, Journal of Materials Science, 24 (1989) 3221-3227.
[16] R.W. Pekala, C.T. Alviso, F.M. Kong, S.S. Hulsey, J. Non-Cryst. Solids, 145 (1992) 90-98.
[17] S.A. Al-Muhtaseb, J.A. Ritter, Adv. Mater., 15 (2003) 101-+.
[18] C.I. Merzbacher, S.R. Meier, J.R. Pierce, M.L. Korwin, J. Non-Cryst. Solids, 285 (2001) 210-215.
[19] H. Tamon, H. Ishizaka, T. Yamamoto, T. Suzuki, Carbon, 37 (1999) 2049-2055.
[20] T. Tsuchiya, T. Mori, S. Iwamura, I. Ogino, S.R. Mukai, Carbon, 76 (2014) 240-249.
[21] M.S. Contreras, C.A. Paez, L. Zubizarreta, A. Leonard, S. Blather, C.G. Olivera-Fuentes, A. Arenillas, J.-P. Pirard, N. Job, Carbon, 48 (2010) 3157-3168.
[22] C. Lin, J.A. Ritter, Carbon, 38 (2000) 849-861.
[23] L. Zubizarreta, A. Arenillas, J. Juan Pis, J.-P. Pirard, N. Job, Journal of Materials Science, 44 (2009) 6583-6590.
[24] L. Zubizarreta, A. Arenillas, J.-P. Pirard, J.J. Pis, N. Job, Microporous Mesoporous Mater., 115 (2008) 480-490.
[25] S.R. Mukai, H. Nishihara, T. Yoshida, K. Taniguchi, H. Tamon, Carbon, 43 (2005) 1563-1565.
[26] H. Nishihara, S.R. Mukai, H. Tamon, Carbon, 42 (2004) 899-901.
[27] I. Ogino, S. Kazuki, S.R. Mukai, Journal of Physical Chemistry C, 118 (2014) 6866-6872.
[28] H. Nishihara, S. Iwamura, T. Kyotani, Journal of Materials Chemistry, 18 (2008) 3662-3670.
[29] Y. Satoh, Y. Yokoyama, I. Ogino, S.R. Mukai, Industrial & Engineering Chemistry Research, 52 (2013) 15293-15297.

Table 1

Textural properties of CMHs, RFs, and RFMHs determined using N_2 adsorption experiments.

Sample	Unidirectional-freezing	Carbonization	S_{BET} [cm^2/g]	V_{micro} [cm^3/g][a]	V_{total} [cm^3/g][b]	V_{meso} [cm^3/g][c]	Peak top [nm][d]	Isotherm
CMH-0-0	○	○	364	0.162	0.168	0.006	1.2	Fig. 2,4,6
RF-0-0[e]	None	None	574	0.244	1.743	1.499	14.1	Fig. 6
RFMH-0-0	○	None	5	0.002	0.015	0.013	22.2	Fig. 6
CMH-0.25-0	○	○	388	0.159	0.310	0.151	5.3	Fig. 2
CMH-0.5-0	○	○	455	0.184	0.433	0.249	6.1	Fig. 2,4,6
RF-0.5-0 [e]	None	None	286	0.113	0.547	0.434	5.3	Fig. 6
RFMH-0.5-0	○	None	213	0.051	0.405	0.354	5.3	Fig. 6
CMH-0-4	○	○	748	0.301	0.578	0.277	2.4	Fig. 8
CMH-0.25-4	○	○	721	0.159	0.310	0.151	5.3	Fig. 8
CMH-0.5-4	○	○	826	0.321	1.115	0.794	6.9	Fig. 8
CMH-0-14	○	○	759	0.286	0.823	0.538	4.6	Fig. 8

[a] Calculated by the DR method. [b] Calculated from adsorbed volume at $P/P_0 = 0.96$. [c] $V_{meso} = V_{total} - V_{micro}$. [d] Peak top position of DH plots.

[e] Freeze-dried after solvent exchange with TBA.

Figure Captions

Fig. 1. SEM images of (a) CMH-0-0, (b) CMH-0.25-0, and (c) CMH-0.5-0.

Fig. 2. (a) N_2 adsorption isotherms and (b) pore size distributions for CMH-0-0, CMH-0.25-0, and CMH-0.5-0.

Fig. 3. SEM images of samples prepared with (a) glucose and (b) dextrin addition.

Fig. 4. N_2 adsorption isotherms of samples prepared with glucose and dextrin addition together with those of CMH-0-0 and CMH-0.5-0.

Fig. 5. High-resolution FE-SEM images of (a) CMH-0-0, (b) CMH-0.25-0, and (c) CMH-0.5-0. The insets represent an enlarged image.

Fig. 6. N_2 adsorption isotherms of samples during preparation of (a) CMH-0-0 and (b) CMH-0.5-0. The adsorption amounts were calculated based on the assumed sample weight from their carbon yield.

Fig. 7. Structural changes during unidirectional freezing of RF hydrogels prepared (a) without and (b) with dextran addition.

Fig. 8. (a) N_2 adsorption isotherms and (b) pore size distributions of CMHs prepared by HCl treatment with addition of various amounts of dextran.

Fig. 1.

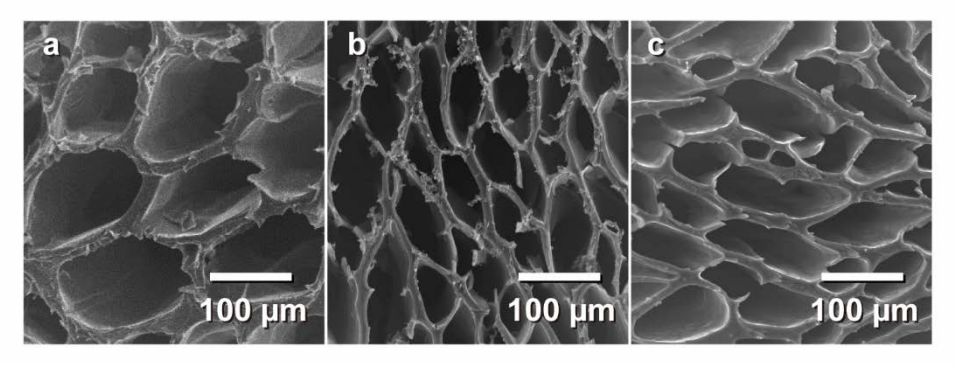

Fig. 2.

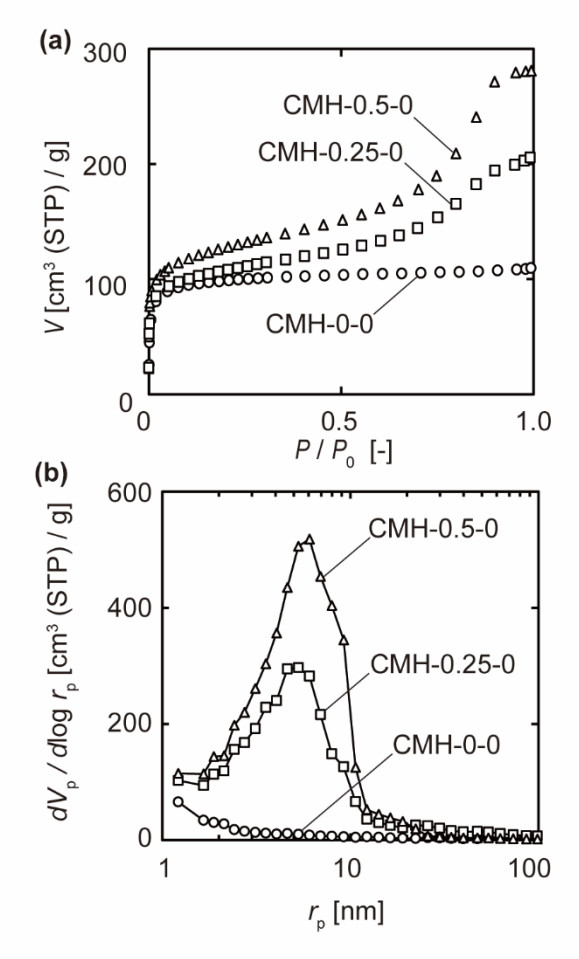
(a)
300
200
100
0
V [cm³ (STP) / g]
CMH-0.5-0
CMH-0.25-0
CMH-0-0
0
0.5
1.0
P / P0 [-]
(b)
600
400
200
0
dVp / dlog rp [cm³ (STP) / g]
CMH-0.5-0
CMH-0.25-0
CMH-0-0
1
10
100
rp [nm]

Fig. 3.

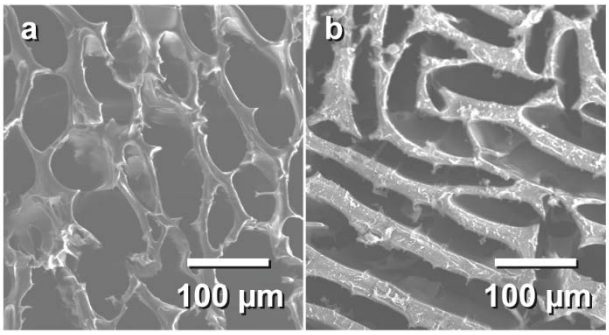

Fig. 4.

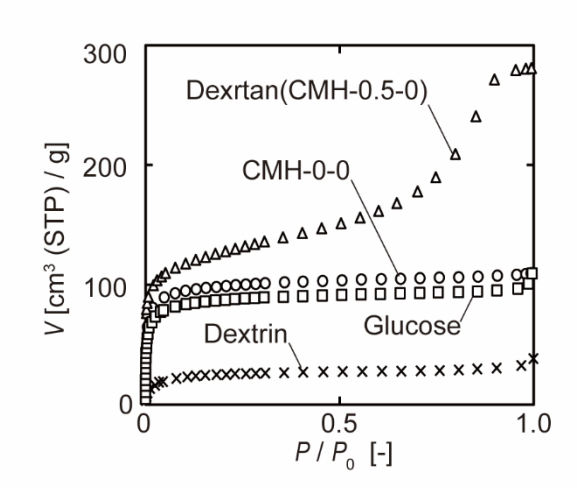
300
200
100
0
V [cm3 (STP) / g]
Dexrtan(CMH-0.5-0)
CMH-0-0
Glucose
Dextrin
0
0.5
1.0
P / P0 [-]

Fig. 5.

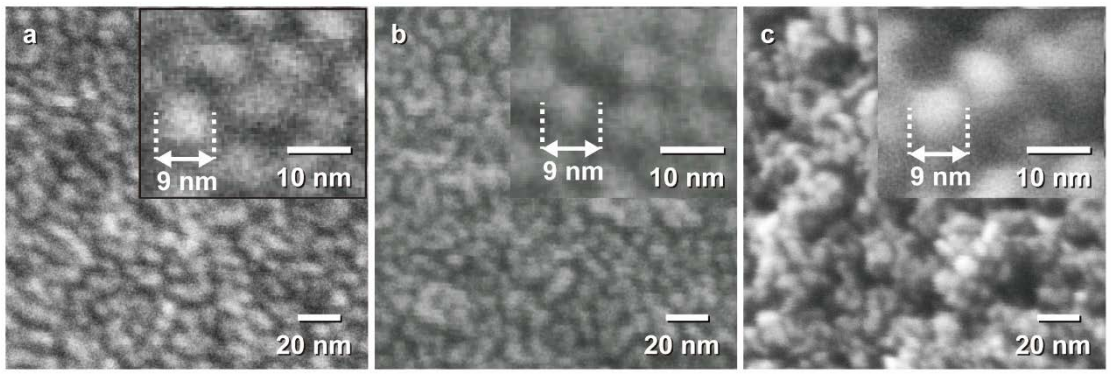

Fig. 6.

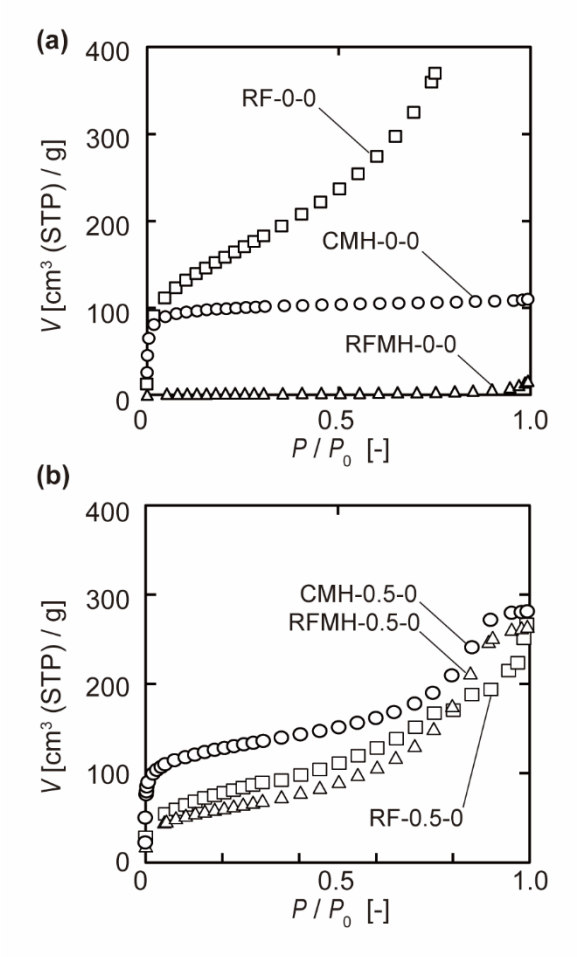
(a)
400
300
200
100
0
V [cm³ (STP) / g]
RF-0-0
CMH-0-0
RFMH-0-0
0
0.5
1.0
P / P0 [-]
(b)
400
300
200
100
0
V [cm³ (STP) / g]
CMH-0.5-0
RFMH-0.5-0
RF-0.5-0
0
0.5
1.0
P / P0 [-]

Fig. 7.

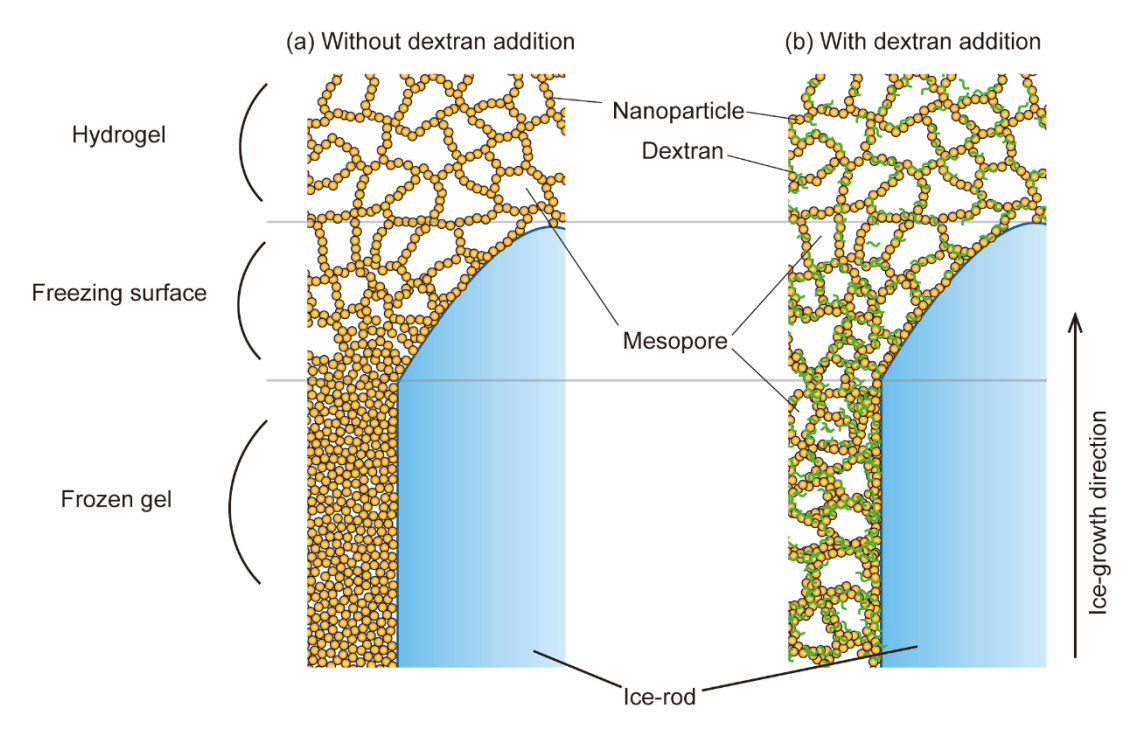
(a) Without dextran addition
(b) With dextran addition
Hydrogel
Freezing surface
Frozen gel
Nanoparticle
Dextran
Mesopore
Ice-rod
Ice-growth direction

Fig. 8.

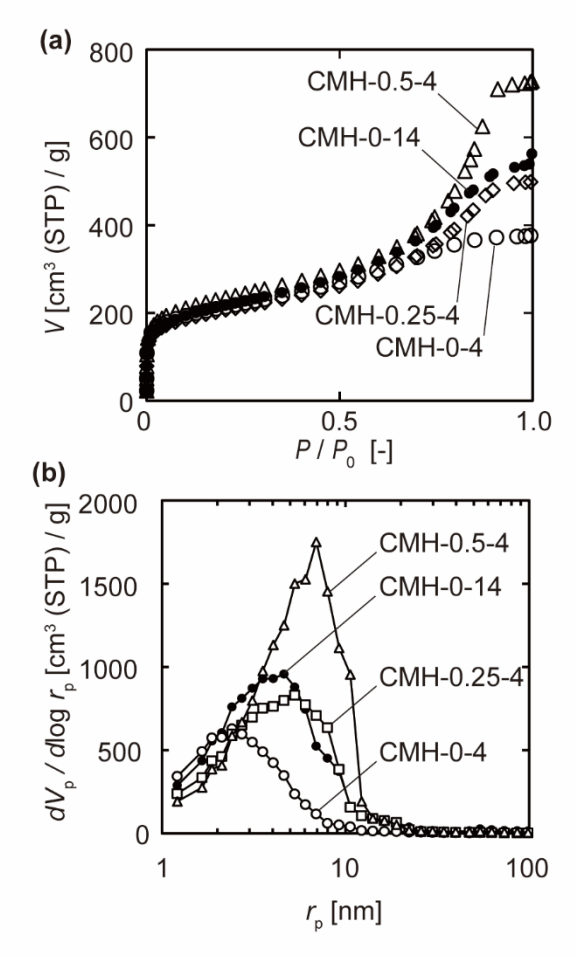
(a)
800
600
400
200
0
V [cm³ (STP) / g]
CMH-0.5-4
CMH-0-14
CMH-0.25-4
CMH-0-4
0
0.5
1.0
P / P0 [-]
(b)
2000
1500
1000
500
0
dVp / dlog rp [cm³ (STP) / g]
CMH-0.5-4
CMH-0-14
CMH-0.25-4
CMH-0-4
1
10
100
rp [nm]